



ORIGINAL PAPER

SURFACE WAVES AS A COST-EFFECTIVE TOOL FOR ENHANCING THE INTERPRETATION OF SHALLOW REFRACTION SEISMIC DATA

Martin MAZANEC^{1,2)} * and Jan VALENTA^{1,2)}¹⁾ Institute of Hydrogeology, Engineering Geology and Applied Geophysics, Faculty of Science, Charles University, Albertov 6, 128 00 Prague, Czech Republic²⁾ Institute of Rock Structure and Mechanics, Czech Academy of Sciences, V Holešovičkách 41, 182 09 Prague, Czech Republic*Corresponding author's e-mail: martin.mazanec@natur.cuni.cz

ARTICLE INFO

Article history:

Received 9 September 2023

Accepted 26 September 2023

Available online 30 September 2023

Keywords:

Surface waves

Rayleigh waves

MASW

Shear wave velocity

Refraction tomography

Ground water level

ABSTRACT

Surface waves typically constitute the dominant component of the seismic record, thus yielding the highest signal-to-noise ratio. Their propagation velocities are closely linked to the shear-wave velocity of the medium. In this study, we provide a review of the basics of surface wave analysis, focusing on Multichannel Analysis of Surface Waves (MASW). We illustrate this approach through four case studies representing common geophysical tasks. By incorporating basic surface wave dispersion analysis into standard refraction surveys, we aim to reduce solution ambiguity and enhance knowledge without incurring additional costs.

In Case Study 1, we address the topic of vertical geophone natural frequencies and compare data acquired simultaneously, concluding that even with 10 Hz geophones, surface wave dispersion analysis can yield satisfactory results.

Case Study 2 demonstrates that MASW analysis can successfully supplement the standard travel-time tomography and help define geological interfaces.

In Case Study 3, we demonstrate that obtaining P-wave and S-wave velocities from a single acquisition setup can aid in determining groundwater level.

Case Study 4 showcases an example of joint passive and active MASW analysis, resulting in an extended shear wave velocity model.

As our four case studies illustrate, when used appropriately and with an understanding of its limitations, MASW can serve as a powerful tool for subsurface investigation across various geological and geotechnical settings, significantly augmenting the knowledge derived from refraction data.

INTRODUCTION

While the highest amount of seismic energy propagates in the form of surface waves, they are still rarely used in routine near-surface geophysical prospecting. Even though surface wave analysis is a classical research field in seismology (Evison et al., 1960; Knopoff and Panza, 1977) and to a limited extent in near-surface geophysics as well (Gabriels et al., 1987; Jongmans and Demanet, 1993), they were generally considered as noise in the past. From today's perspective, a significant breakthrough in this field was the work of Park et al. (1998, 1999), who introduced an effective and straightforward method for processing surface waves, commonly known as Multichannel Analysis of Surface Waves (MASW). Since then, the number of articles describing their usefulness has dramatically increased; however, not many practitioners still recognize the benefits they bring. This article aims to demonstrate, through four case studies representing common geophysical tasks, how the inclusion of surface waves into standard refraction surveys could reduce solution ambiguity

and expand the obtained knowledge at no additional cost.

The seismic wave energy propagates predominantly as surface waves, either Rayleigh waves (oscillating in vertical and horizontal plane and hence detectable with vertical seismic sensors) or Love waves (oscillating in horizontal plane and thus requiring horizontal sensors). Although combination of both Rayleigh- and Love-wave microtremor methods could severely reduce ambiguities and improve the results (Dal Moro and Ferigo, 2011) the need of horizontal geophones, uncommon in most shallow seismic surveys, limits the usefulness of this approach. Therefore, the most common approach is using vertical sensors limiting the processing and interpretation to Rayleigh waves (Rw) analysis (Foti et al., 2018); hence, we also confine the discussion to this category.

The utmost contribution of Rayleigh wave processing is determination of S-wave velocities (although on 1D model only). The changes in S-wave velocities are more sensitive to mechanical

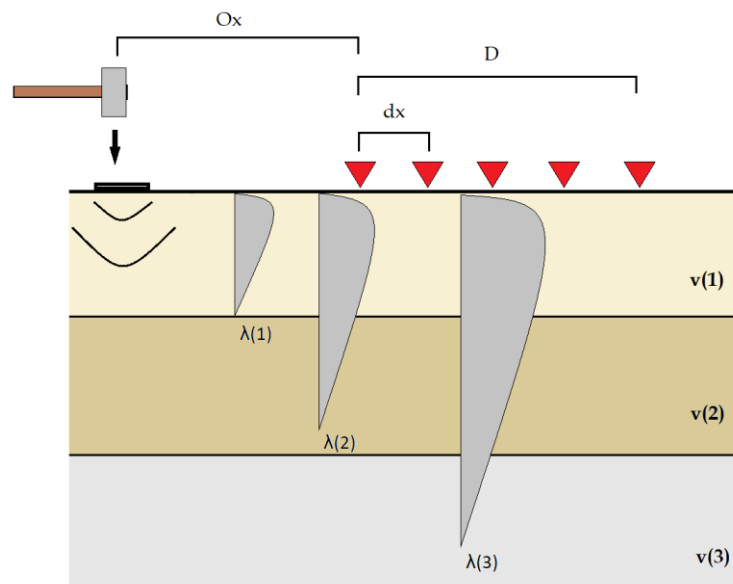


Fig. 1 Multichannel acquisition scheme showing seismic source (a sledgehammer), geophones (red triangles), source offset (O_x), length of the receiver spread (D) and receiver spacing (dx). Different wavelengths ($\lambda(x)$) of Rayleigh waves propagate from the source through a layered medium (where each layer has a different velocity $v(x)$) with a different depth of penetration.

disintegration of the geological environment then changes in P-waves (Barton, 2006) and their combination in the form of P/S wave ratio could be of utmost importance for hydrogeologists as one of the few methods for direct identification of ground water level (Pasquet et al., 2015). Another parameter which could be obtained from surface wave propagation is the quality factor Q_s (Zhou et al., 2020) although the complex effect of attenuation and dispersion could increase the uncertainty (Vavryčuk, 2008).

The interpreted data comprise surface wave velocity spectra aimed at defining the phase (Lai, 1998; Park et al., 1998; Ohori et al., 2002) or group velocities (Ritzwoller and Levshin, 1998; Kolínský et al., 2014). As shown in Figure 1, to achieve deep penetration, long-wavelength (low-frequency) data are required. Therefore, high-frequency active data (energy generated, for example, by a hammer strike) can be supplemented with low-frequency, long-wavelength passive data (recording of low-frequency noise) and processed simultaneously (Tokimatsu et al., 1992a; Park and Miller, 2005; Park et al., 2007).

Currently, the most common method of surface wave processing is the Multichannel analysis of surface waves (MASW) introduced by Park et al. (1998, 1999). While this method may appear robust it has several shortcomings mainly connected with presence of higher modes which can lead to erroneous V_S profiles determination (Dal Moro, 2023 and references therein). However, it is possible to overcome this problem by recording both, vertical and horizontal vibrations, and obtain reliable V_S profiles (Dal Moro, 2014, 2020; Dal Moro and Ferigo, 2011). Nevertheless, multi-component observations demand multi-component geophones or multiple types of

geophones further complicating the survey. In this context, we focused on the simplest approach suitable as an add-on to a standard refraction survey.

The MASW was recognized as an efficient method for elastic property of near-surface materials investigation and has found wide applications such as bedrock mapping (Miller et al. 1999; Park 2016), marine environments investigation (Kaufmann et al., 2005), hydrogeological studies (Suto, 2012; Pasquet et al., 2015), landslides (Suto et al., 2016; Strelec et al., 2017), liquefaction potential analysis (Lin et al., 2004), karst investigation (Debeglia et al., 2006), geotechnical site characterization (Penumadu and Park, 2005; Park, 2013; Abudeif et al., 2019) etc. MASW has also become very common tool for average shear wave velocity in the upper 30 m (V_{S30}) determination (Gaytan et al., 2020; Sairam et al., 2019; Hollender et al., 2018; Odum et al., 2013; Foti et al., 2011). Kanli et al. (2006) were using MASW for V_{S30} mapping and soil classification in Turkey, Rahman et al. (2018) estimated V_{S30} in 151 sites in Dhaka, capital city of Bangladesh using MASW as one of the methods.

MULTICHANNEL ANALYSIS OF SURFACE WAVES

Because of its simplicity and easy adoption, we focus here on the Multichannel analysis of surface waves (MASW), first introduced by Park et al. (1999). This method utilizes dispersion property of surface waves for the purpose of V_S profiling. It has found many useful applications so far (e.g., Xia et al., 2002; Socco et al., 2010). In most cases, the processing is based on the analysis of the vertical component of Rayleigh waves, as they are easy to generate and detect although the Love waves could be used as well

(Dal Moro and Ferigo, 2011). The active MASW is often the preferred approach, also because of the ability to control the source offset (Fig. 1). The most common frequency range in the active survey is between the 5-50 Hz (Park et al., 2002). When a deeper penetration is needed, the passive MASW allows extending the depth reach by recording low frequency components (<5-7 Hz) (Park and Miller, 2005). A combination of the both approaches – the joint analysis of passive and active MASW (Dal Moro, 2020) – we will discuss further in the text.

The standard active or passive MASW process uses vertical component of Rayleigh waves and consists of the following steps: (i) a multichannel records acquisition, (ii) dispersion analysis and (iii) inversion analysis leading to the V_s profile. In the active MASW method the surface waves are generated using an impact source (usually a sledgehammer). Whereas in the passive MASW approach (also called e.g., Microtremor Array Method), the source of surface waves are natural or artificial ambient vibrations (Aki, 1957; Tokimatsu, et al., 1992a). The main advantage of passive MASW are low frequency waves recorded and thus a deep penetration of the survey.

(i) ACQUISITION

The acquisition is done by a multichannel linear array consisting of low frequency vertical receivers, most common are the 4.5 Hz geophones. Maximum investigation depth (Z_{max}) is generally determined by the longest possible analysed wavelength λ_{max} (Fig. 1):

$$Z_{max} = 0.5 \lambda_{max} \quad (1)$$

and by the length of the receiver spread (D), which is directly related to λ_{max} and usually should be equal to or greater than Z_{max} :

$$D = mZ_{max} \quad (1 \leq m \leq 3) \quad (2)$$

However, in active MASW the length of the profile also depends on the energy of seismic source and its offset (O_x , Fig. 1) as the surface waves generated by most active sources could easily become attenuated below a noise level at the far end of the receiver spread (so called *far-field effects*). In addition, the large values of the O_x and D increase the risk of higher-mode domination and reduce the fundamental mode S/N. However, O_x must be sufficiently large to avoid a *near-field effect*. This effect occurs when a seismic source is located too close to the receiver array and the recorded signal is significantly altered, resulting in distorted waveforms. Dal Moro (2014) specifically recommends choosing a source offset between 5 and 20 m. A vertical stack (summation) of traces from multiple shots is recommended to suppress incoherent noise.

Receiver spacing (d_x) is related to the shortest wavelength (λ_{min}) and therefore determines the shallowest resolvable depth of investigation (Z_{min}):

$$Z_{min} = kd_x \quad (0.3 \leq k \leq 1.0) \quad (3)$$

Dal Moro (2014) also shows that the number of channels to use for the MASW is not that relevant and should be kept between 12 and 24.

For MASW surveys that utilize an impact point load to generate surface waves, the typical recording time (T) is 1-2 seconds. It is crucial to ensure that the entire surface wave signal is fully recorded across all channels. For near-surface geological applications, a sampling interval of 1 millisecond is generally adequate.

The passive MASW method adopts the conventional linear receiver array or other offline geometry types such as circle, cross, square, triangular, etc. As noted by Park (2007) an array of significant asymmetric shape is not recommended due to bias toward a specific direction of incoming surface waves.

The above-mentioned general rules for acquisition parameters are based on several independent studies (Park et al., 1999; Park et al., 2002; Park and Carnevale, 2010; Dal Moro, 2014; Foti et al., 2014; Olafsdottir, 2016) and are intended solely for initial orientation. Practitioners should be familiar with the geological context of the investigated site, always start the survey with a test measurement and adjust the acquisition geometry accordingly.

(ii) DISPERSION ANALYSIS

The objective of dispersion analysis is to estimate dispersion curve(s) (DC) that represent the dispersion image and will be used in the next step as input for the inversion process. Dispersion analysis itself consists of two steps. The first step involves generating a dispersion image (Fig. 2b) from acquired seismic records (Fig. 2a) using one of the wavefield transformation method, e.g., the frequency–wave number (f – k) transform (Yilmaz, 1987), the slowness–frequency (p – ω) transform (McMechan and Yedlin, 1981) or the phase shift method (Park et al., 1998). The latter is the most common approach and as noted by Dal Moro et al. (2003), who compared the aforementioned techniques, the phase shift method stands out as a robust and effective technique, providing accurate fundamental mode phase velocities, even with a limited number of receivers.

For passive surface wave processing, the spatial autocorrelation (SPAC, Aki, 1957) and f - k methods are commonly used. Furthermore, Park et al. (2004; 2007) developed an imaging method similar to the one used in the active MASW. Nevertheless, the SPAC is one of the most commonly used methods because of its robustness, ease of implementation, and computational efficiency Hayashi et al. (2022).

In the generated dispersion image different modes of surface wave propagation are recognized by their frequency content and characteristic phase velocity at each frequency. The second step of the dispersion analysis is to extract from the dispersion image the most representative dispersion curve(s)

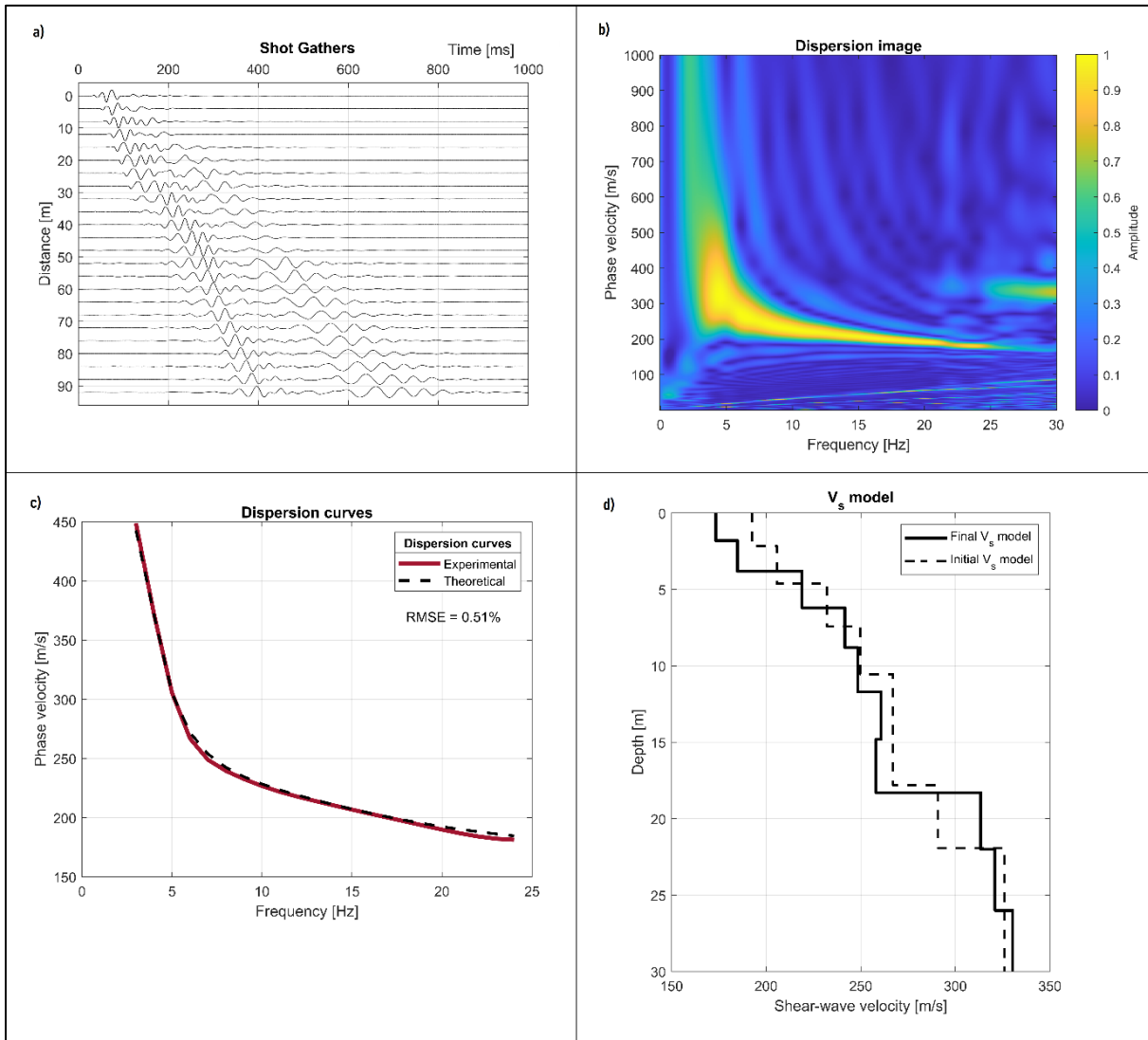


Fig. 2 Overview of the MASW: a) Multichannel waves propagation record (shot gathers); b) Rayleigh waves dispersion image where the fundamental mode (yellow amplitudes) clearly dominates; c) the experimental (red line) and theoretical (black dashed line) fundamental mode dispersion curves of the inverted shear wave velocity model (d). Goodness of fit between both dispersion curves is characterized by the RMSE. Figure d) shows both initial (dashed line) and final (solid line) V_s models. This real data analysis example was recorded at a site dominated by quaternary sediments (loess and gravel beds).

(Fig. 2c). Socco et al. (2010) summarized and discussed two main approaches dealing with the dispersion curve(s) extraction: (1) using only fundamental mode (M0) and (2) multi-modal approach using not only M0 but also higher mode(s) of propagation. Apparent (effective) dispersion curve (Tokimatsu et al., 1992b; Lai et al., 2014) is an example of the latter. The most common approach is using only Rayleigh wave fundamental mode dispersion curve as it usually dominates in the seismic record. With this approach practitioners need to be aware of potential risks such as not clear dispersion image or higher mode dominance (e.g., Tokimatsu et al., 1992b; Dal Moro, 2023). This extracted curve is called an *experimental* dispersion curve and is an input data to the next (iii) inversion analysis step.

(iii) INVERSION

The inversion analysis involves obtaining a shear wave velocity profile (Fig. 2d) by inversion of the *experimental* dispersion curve. The whole process starts by creating an initial V_s model (Fig. 2d) for which the *theoretical* dispersion curve is calculated and compared to the *experimental* DC. Based on curves difference the initial V_s model is modified. For the new model a new *theoretical* DC is calculated. This iterative process continues until the *theoretical* curve matches reasonably well with the *experimental* DC which is defined by the root means square error (RMSE). As reports Olafsdotir (2016) the inversion analysis contains three fundamental components (1) optimization technique to estimate an initial set of model parameters; (2) algorithm to compute

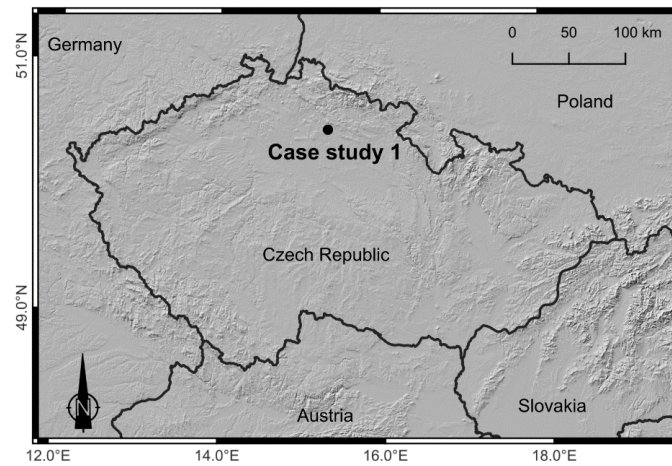


Fig. 3 Case study 1 site map.

theoretical dispersion curves from assumed layered model; (3) algorithm to evaluate and minimize the misfit between the *theoretical* and the *experimental* dispersion curves. Here the most important difference is between global search methods (GSM, application examples included in Socco et al., 2010), and local search methods (LSM, e.g., Xia et al., 1999). The final shear wave velocity profile is the result of all three steps (i-iii) of the MASW analysis.

CASE STUDIES

In the following chapter, we explore the possibilities and advantages of using MASW in

shallow seismic surveys, alongside standard seismic refraction tomography. We present four case studies, each representing a common geophysical task where surface wave analysis was employed as a complementary method, greatly improving and enhancing the standard tomography.

CASE STUDY I

Geophones are usually specified by their natural frequency, i.e., the frequency at which the mass inside the geophone naturally oscillates. For surface-wave studies the low frequency geophones (e.g., with 4.5 Hz natural frequency) are generally recommended to

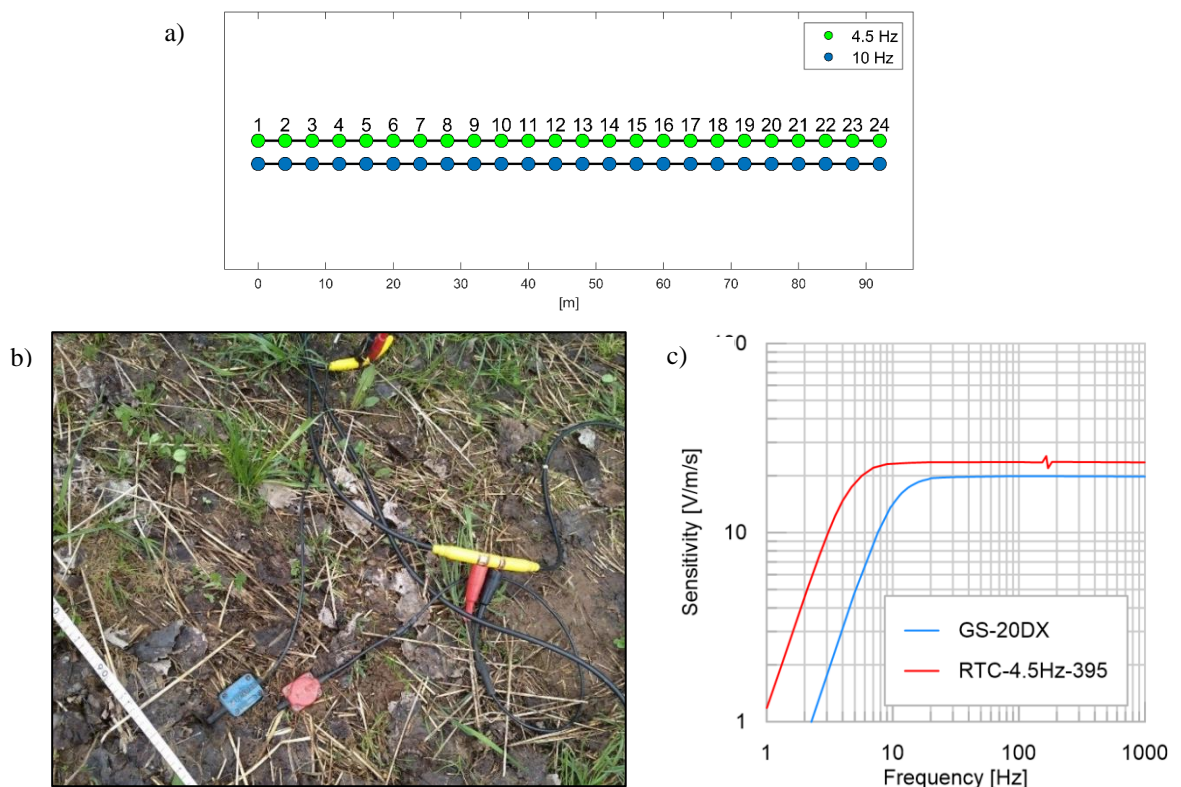


Fig. 4 Geophone array geometry (a), the acquisition setting showing close positions of both 4.5 Hz (red) and 10 Hz (blue) vertical geophones (b), response curves for 4.5 Hz, and 10 Hz geophones used in the test (c).

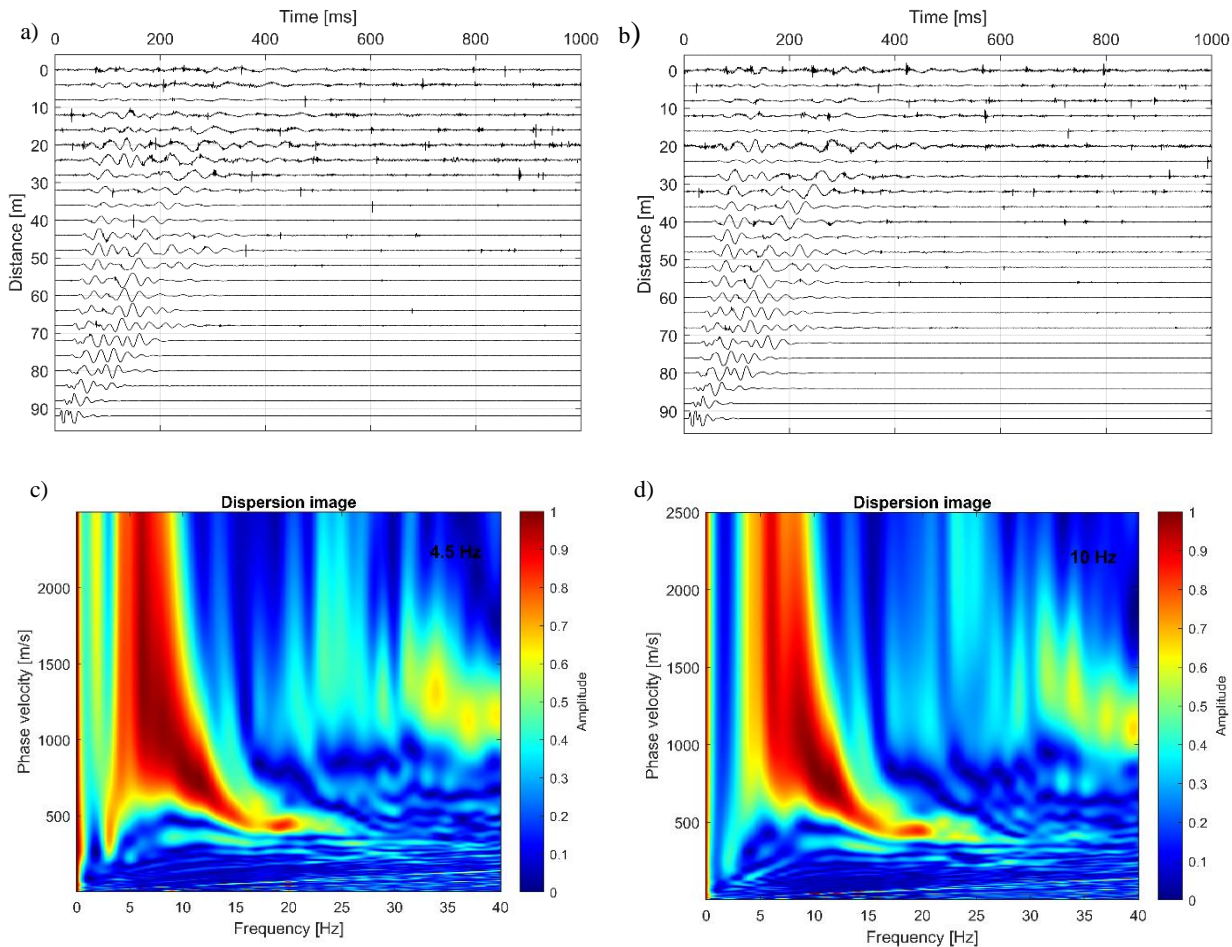


Fig. 5 Shot gathers (a and b) from the 94 m shot position, surface waves dispersion images (c and d), both for 4.5 Hz (left panel) and 10 Hz (right panel) geophones.

record the long-wavelength deep penetrating part. However, not many practitioners use geophones with such low natural frequency, instead, the 10 Hz geophones are more common in shallow seismic refraction. The aim of the Case study 1 is to demonstrate that even the 10 Hz geophones can be used for such research. In the first case study we show comparison of two seismic datasets from the same seismic profile. The site was situated in the landslide zone in north-east Bohemia (Fig. 3). Seismic refraction data were acquired simultaneously using two types of vertical geophones with different natural frequency - 4.5 Hz (RTClark geophones RTC-4.5Hz-395) and 10 Hz (Geospace, GS-20DX). As shown in the Figure 4b both types of geophones were placed at the same positions of the seismic profile in the very close proximity to each other so that their recordings are comparable.

Seismic profile was 92 m long with 4 m geophones spacing (24 geophones of each type were used in total). Refraction data were acquired using 10 kg sledgehammer shots on a metal plate every 8 meters of the profile. To achieve a high signal/noise ratio for the surface waves analysis, 8 vertically

stacked shots were performed in the shot points at both ends of the profile. The length of the seismic records was 1 sec to record all generated wave types (Fig. 4a).

Figure 4c illustrates response curves for the geophones used in this study. As stated in Dean and Shem (2018) the 4.5 Hz and 10 Hz geophones differ substantially only in their natural frequencies not in the sensitivity. It is evident from the chart that below the natural frequency the sensitivity decreases rapidly. E.g., at 5 Hz the signal from the 4.5 Hz geophone is roughly three times larger than signal from the 10 Hz geophone. Nevertheless, the signal from the high-frequency geophone can still be recovered with the cost of a lower S/N ratio.

To compare the two acquired datasets (from 4.5 Hz and 10 Hz vertical geophones) and show that surface waves analysis can be easily performed on the refraction data, we show in Figure 5 data from the seismic source shot position 94 m acquired with both types of geophones. Top panel (a and b) shows seismic shot gathers of both datasets. The two records are very similar, both in arrival times and amplitudes. They do not differ significantly in noise either. Lower panel (c and d) refers to surface waves dispersion images

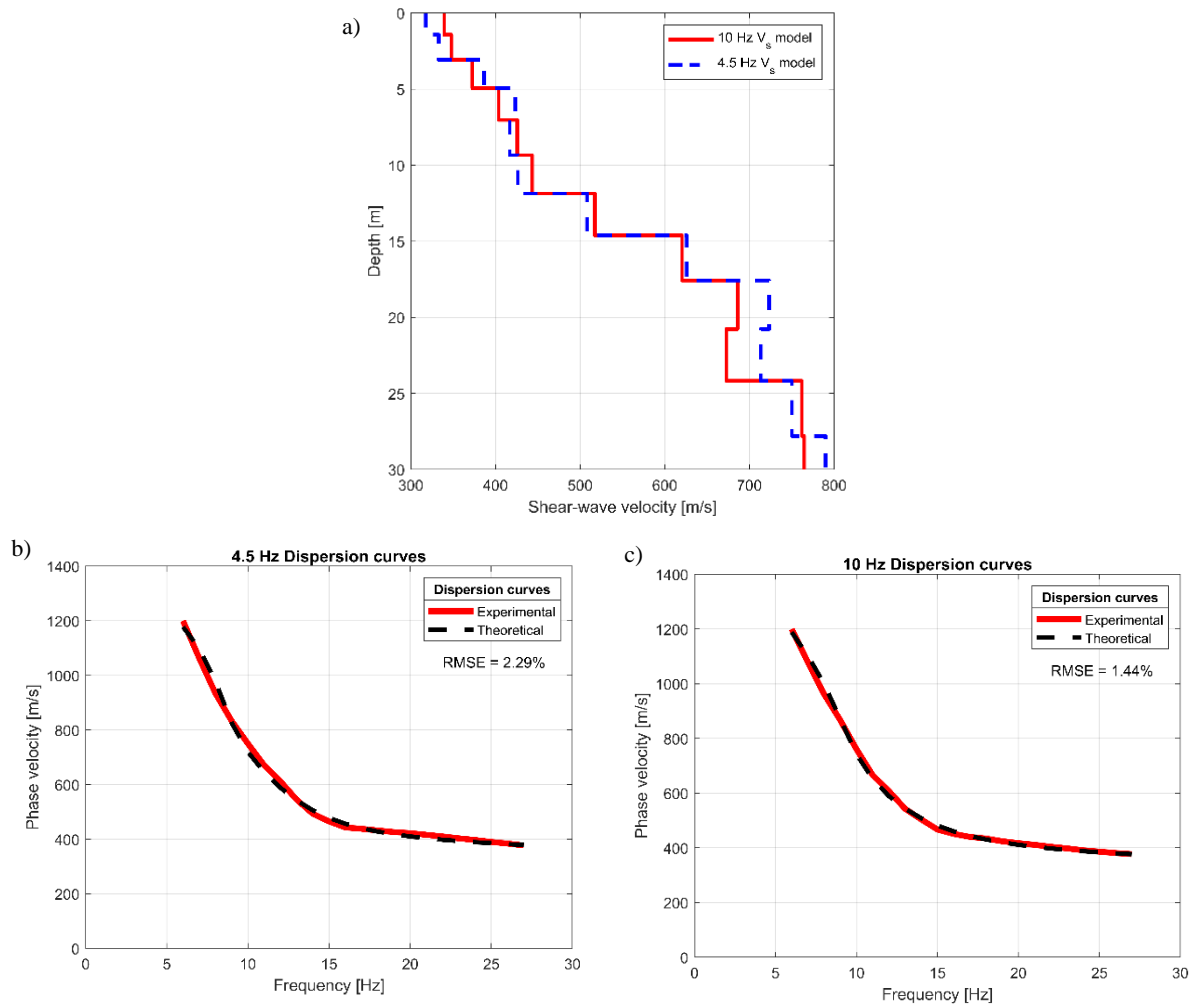


Fig. 6 Final V_s models (a) for both 4.5 Hz (blue dashed line) and 10 Hz (red solid line); (b) 4.5 Hz and (c) 10 Hz theoretical (black dashed line) and experimental (red solid line) V_s models' associated dispersion curves and RMSE for both datasets.

obtained using Phase-Shift method (Park et al., 1998). The pattern of both dispersion spectra is identical, with the 4.5 Hz geophones spectrum showing higher amplitudes in the low frequency zone around 5 Hz. In addition, the presence of higher mode(s) is more visible in 4.5 Hz dataset. On the other hand, the 10 Hz spectrum indicates higher amplitudes in the 20-30 Hz frequency zone providing easier characterization of the fundamental mode dispersion curve at higher frequencies and thus refining the shallow part of V_s model. Nevertheless, both datasets are very similar in the sense of recorded traces as well as the dispersion image.

Next, fundamental mode dispersion curves of both datasets were picked and inverted into final V_s models using the non-linear least squares method (LSM) (Fig. 6a). Thirty meters of both V_s models are plotted in a single figure (red line refers to the 10 Hz geophones dataset and blue dashed line refers to the 4.5 Hz geophones dataset) so that they can be compared. In the shallowest parts 0-5 m both V_s

models follow the same trend with gradually low ascending velocity and their difference does not exceed 20 m/s. In the 5-11 m section the 4.5 Hz model shows a minute velocity inversion whereas the 10 Hz model continues in the ascending velocity trend. In the following section 11-17 m both models are almost identical with minor differences up to 10 m/s. From 17 to 24 m both models follow the same trend with velocity inversion in the depth 20.8 m and subsequent velocity increase. The velocity variations here are larger, up to 40 m/s. In the deepest V_s models' section 24-30 m the 4.5 Hz dataset shows a more significant velocity increase than the 10 Hz, however the velocity values vary only by a maximum of 25 m/s.

It can be seen that both velocity models are very similar with differences in the order of percentages. Both are following the same trend with several significant velocity drops (especially 11.8 m, 14.6 m, 17.6 m) and bland velocity inversion (20.8 m). Figures 6b and c show V_s models' associated experimental and theoretical dispersion curves. The

RMSE for the 4.5 Hz dataset is 2.29 % and 1.44 % for the 10 Hz dataset. The shape and velocity range of the two experimental curves highlights the similarity of the two datasets.

The obtained results confirm that for basic dispersion analysis of surface waves, besides the recommended 4.5 Hz geophones (and possibly even lower natural frequency geophones), the standard 10 Hz geophones common in the shallow refraction seismic can be used as well. As shown in Figure 5 the differences in the recordings and dispersion spectra of these two types of geophones are insignificant. Figure 6 confirms this insistence as it shows that the resulting 30 m Vs models (and DCs) obtained from the 4.5 Hz and 10 Hz datasets are very similar. Naturally, their difference will increase with the depth as the sensitivity of geophones rapidly decreases below their natural frequency. In addition, dispersive analysis of surface waves can be used retrospectively on already existing refraction data (if the dataset is suitable), thus reducing the ambiguity of the solution.

CASE STUDY 2

The result of the MASW is usually a 1D Vs model. Although the model describes only horizontal interfaces it can give a fundamental information for interpreting 2D or 3D models, results of other geophysical methods. The Case study 2 was focused to determine depth of weathering in the vicinity of the Benešov town (Fig. 7) as a part of the geological survey for construction of a new motorway.

The geological background on the site was mainly composed of granitic rocks of the Central Bohemian Pluton. The granites and granodiorites are deeply weathered with weathering residua *in situ*, making it difficult to determine a weathering boundary.

In this situation, often the shallow seismic refraction is the geophysical method of choice, because the change in velocity of seismic waves is the most reliable quantifier of the rock quality (e.g., Barton, 2006). However, the conventionally applied

P-wave tomography may not always give satisfying results, especially when there a high thickness of *in situ* weathering residuum is present (Fig. 8). The smooth gradient resulting from the tomography processing does not help in interpretation. Nevertheless, the S-waves are much more sensitive to lithological changes and to rock disintegration and weathering than the P-waves (particularly, as described by Barton (2006), because they are not affected by changes in water saturation). Therefore, obtaining the S-wave velocity profile is extremely valuable in this case.

The easiest way of determining the S-wave velocities is from the dispersion curve of Rayleigh waves, although the result is only 1D. As showed in the Case study 1 the dispersion curve can be easily obtained from the field data measured for the tomography processing if the fundamental requirements for the surface waves analysis (listed above) are met. Here we analyse the refraction datasets from profiles 3A and 4 both acquired with 10 Hz geophones with 2s long records and a sledgehammer as a seismic source. Therefore, the refraction tomography data acquired in the field can be used for both analysis with no additional cost.

The result of the surface waves processing is a 1D model and therefore it is advisable to select for analysis only those parts of the profiles where the environment is close to the 1D model. In this Case study 2, these parts were the west part of the profile 3A up to the x-coordinate 115 m and the SE part of the profile 4 from the x-coordinate 115 m further (Fig. 8). Example shot gather from both profiles as well as dispersion images are plotted in Figure 9 and resulting S-wave profiles for these two intervals are plotted in Figure 10. In contrast to P-wave tomography the results clearly show three distinct velocity interfaces each marking substantial changes in elastic properties of the subsurface. Comparing the depth to these interfaces with tomography profiles these interfaces could be approximated by certain P-wave velocity contour lines (in this case the following contour lines

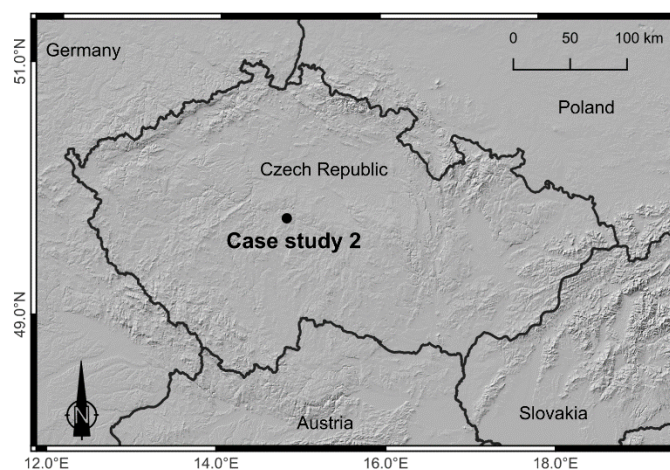


Fig. 7 Case study 2 site map.

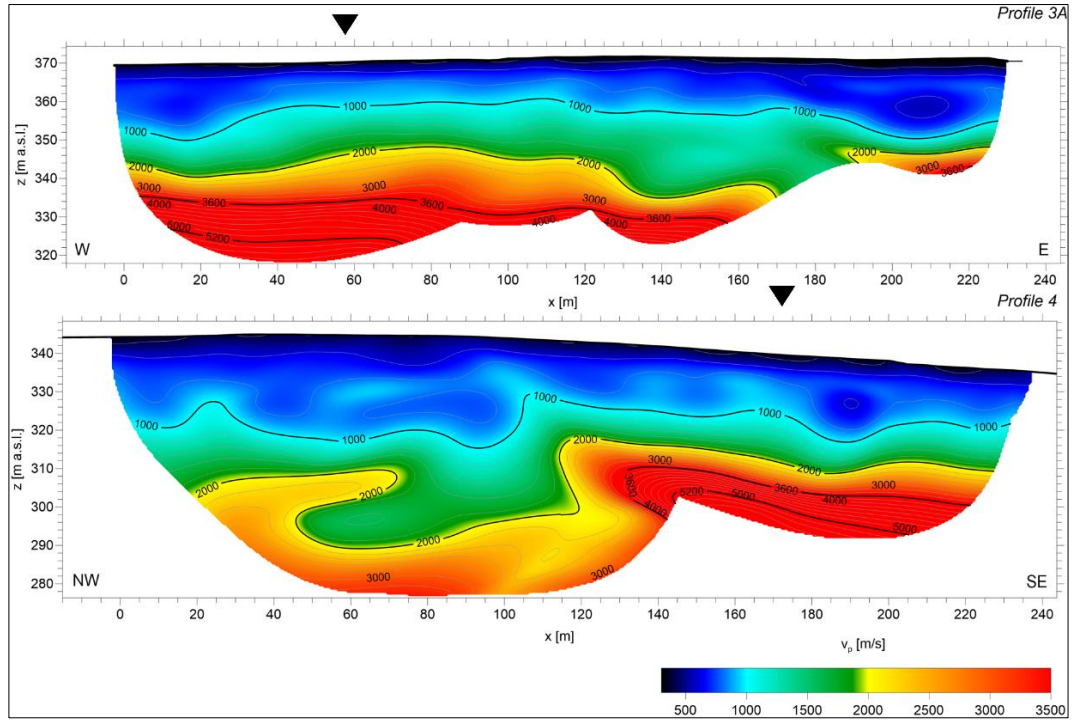


Fig. 8 P-waves travel time tomography models of profile 3A (top) and profile 4 (bottom). Black triangles show 1D Vs models positions. Note the smooth velocity change making it difficult to determine the depth of the weathering interface. The heavy lines of velocity contour lines (1000, 2000, 3600 and 5200 m/s) approximate interfaces determined from S-wave velocity profiles.

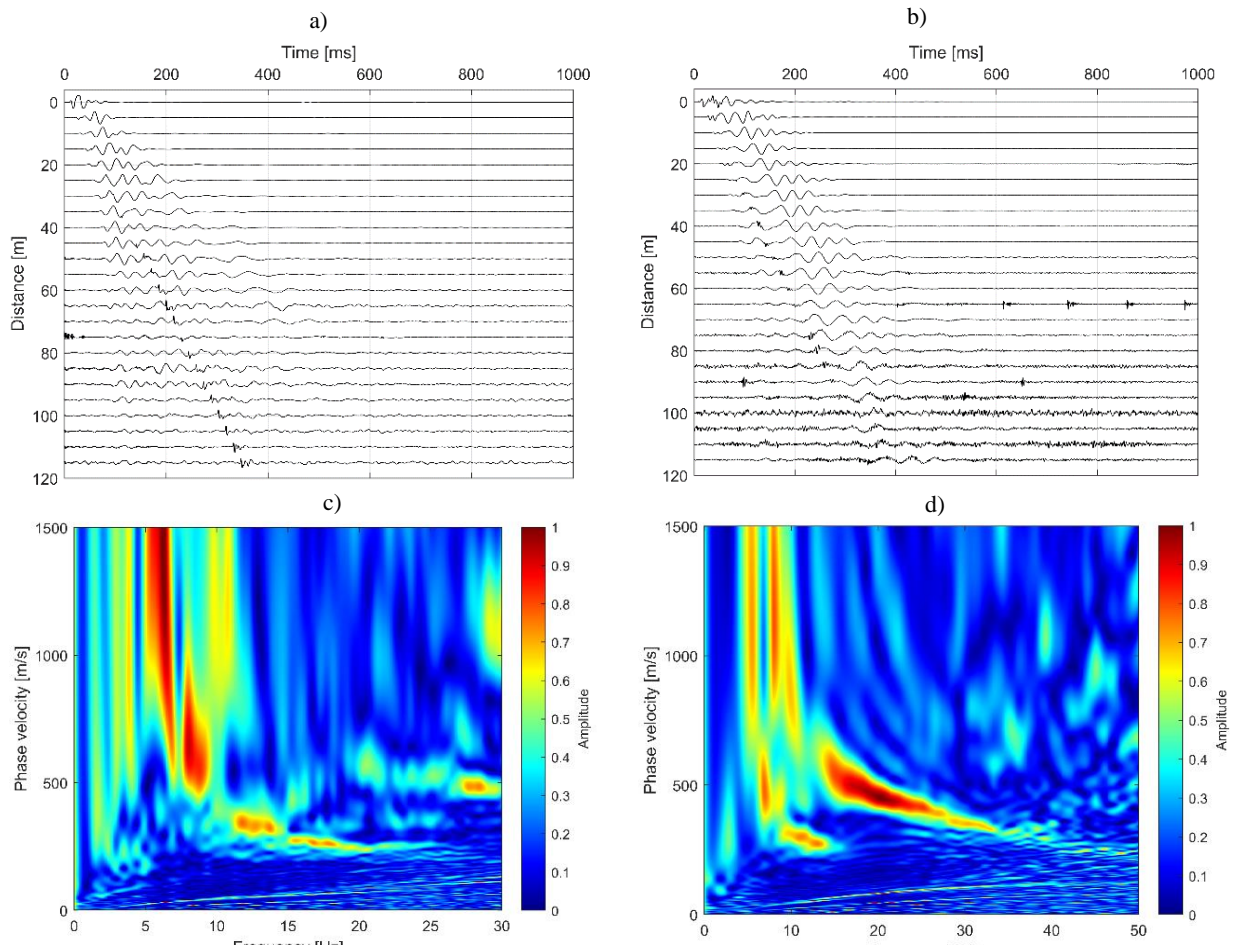


Fig. 9 Example of shot gathers -2.5 m from profiles P3A (a) and P4 (b); (c) and (d) dispersion image Phase shift transformed from the (a) and (b) shot gathers.

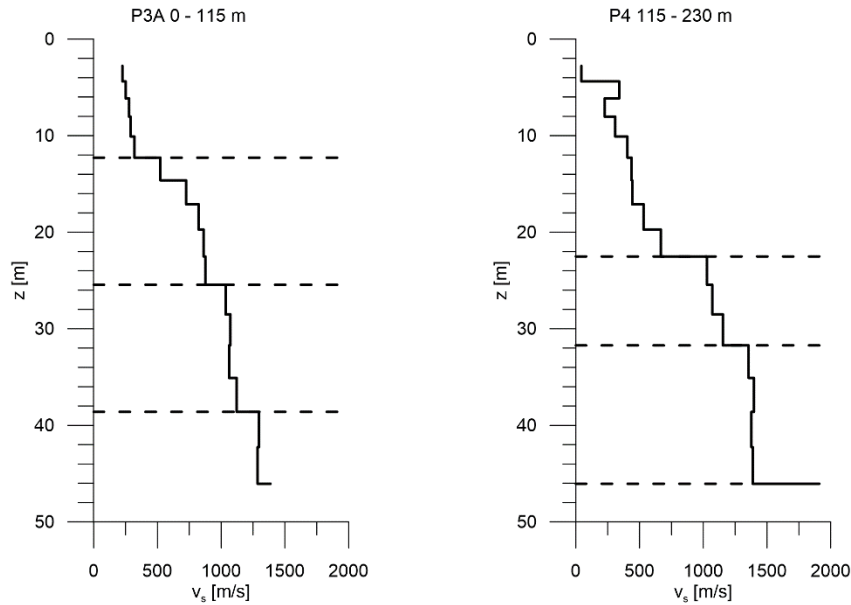


Fig. 10 S-wave velocity models determined from Rayleigh waves for selected parts of the tomography profiles from Figure 8. The horizontal dashed lines mark distinct velocity interfaces.

were used: 1000, 2000, 3600 and 5200 m/s) and extrapolated to remaining parts of the profiles marking the completely weathered, partly weathered and sound granodiorites. These three categories can be roughly estimated from the S-wave velocities (approximately below 500 m/s, 500–1300 m/s, more than 1300 m/s).

CASE STUDY 3

Characterisation and monitoring of groundwater resources are mostly dependent on the presence of boreholes. However, their spatial distribution is generally sparse and drilling a new borehole is relatively expensive. As shown by Pasquet et al. (2015), geophysics can provide supplementary information and expand the understanding of aquifer systems using the joint analysis of pressure and shear wave velocities (V_p and V_s) especially by estimation of V_p/V_s or Poisson's ratios (Stümpel et al., 1984; Bachrach et al., 2000; Barton, 2006). Pasquet et al. (2015) carried out such seismic surveys under two

hydrological conditions and concluded that both V_p and V_s models are consistent with the local (known from the borehole) stratification and V_p/V_s and Poisson's ratios show a satisfactory contrast for both flow regimes at depths consistent with the water table level. Konstantaki et al. (2013) highlighted in their study significant variations of V_p/V_s and Poisson's ratios that associated with the water table level. Recent studies confirmed that the evaluation of these ratios can be systematically carried out with refraction tomography using both P and SH waves (Turesson, 2007; Grelle and Guadagno, 2009).

In the Case study 3 we illustrate how surface waves obtained as a part of refraction data acquisition can easily serve as a useful tool for hydrogeological study. The data considered for the present case study were recorded near the Velké Chrásťany village in SW Slovakia (Fig. 11). The site is situated in the Pliocene Volkovce Formation (Joniak et al., 2020) dominated by sands, gravels and clays. The lithological profile

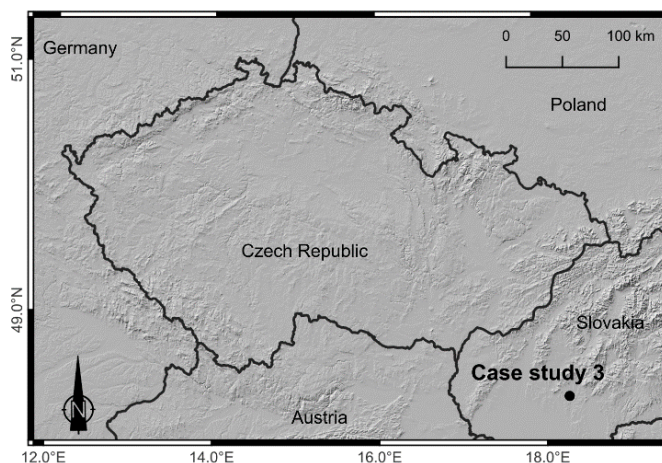


Fig. 11 Case study 3 site map.

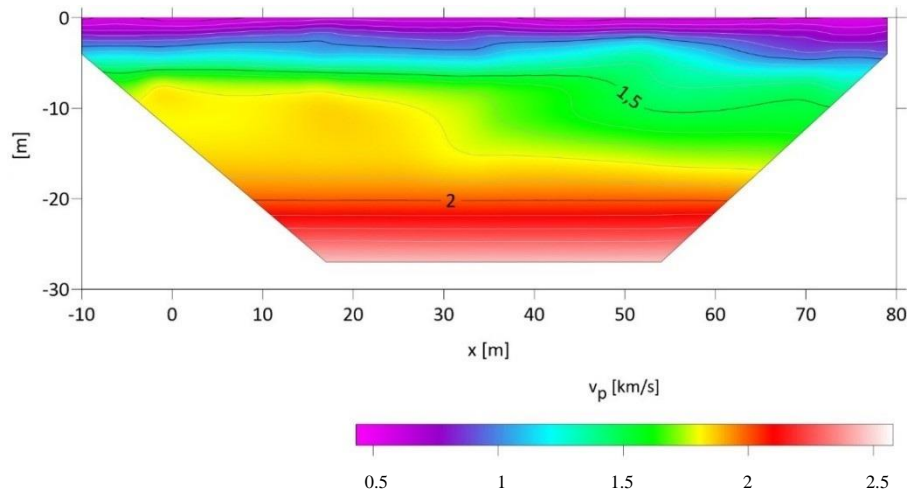


Fig. 12 P-wave travel time tomography model.

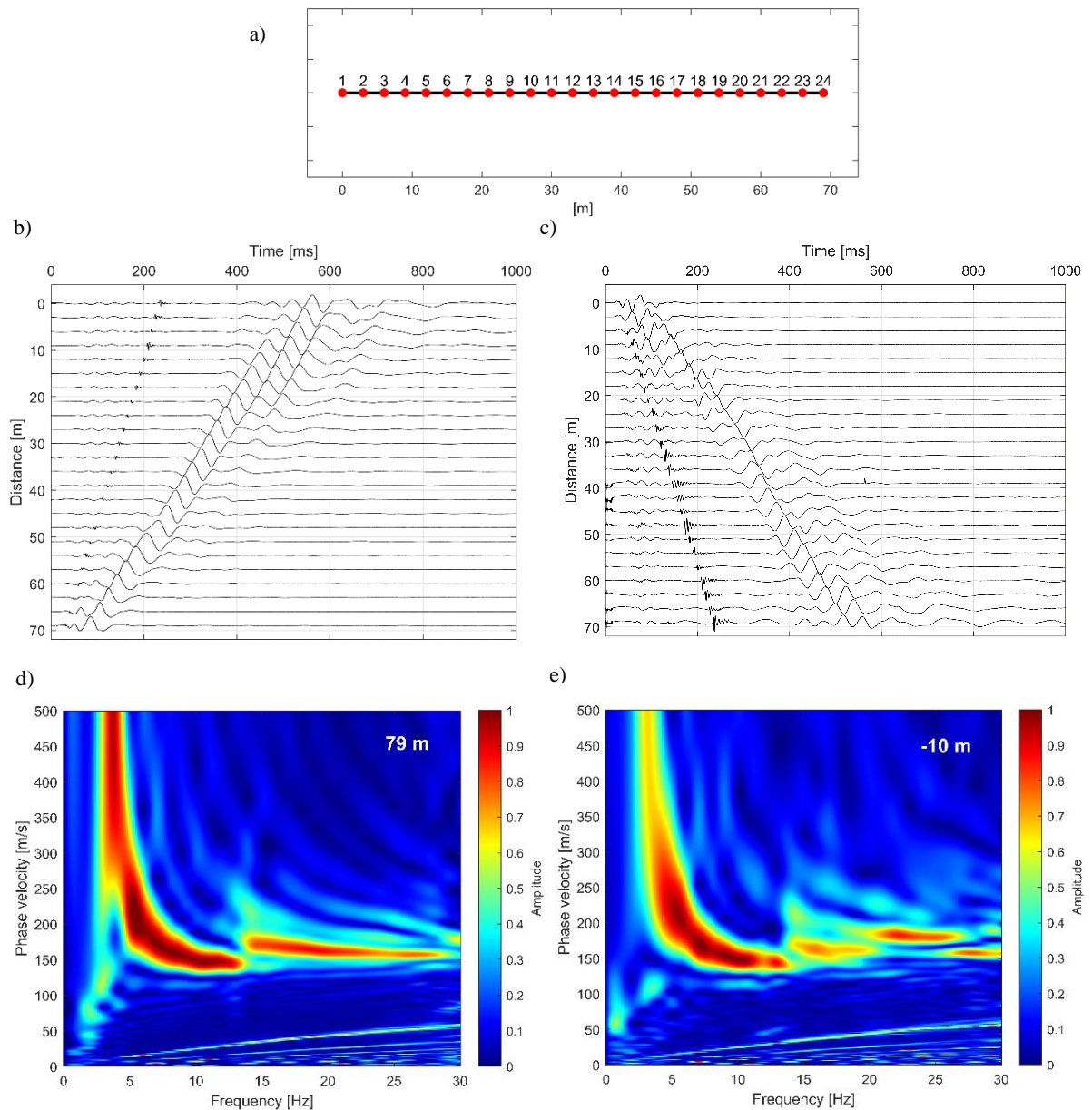


Fig. 13 (a) Seismic array geometry - 24 geophones with 3 m spacing; (b) and (c) shot gathers for 79 m and -10 m shot positions; (d) and (e) dispersion images for 79 m and -10 m shot positions.

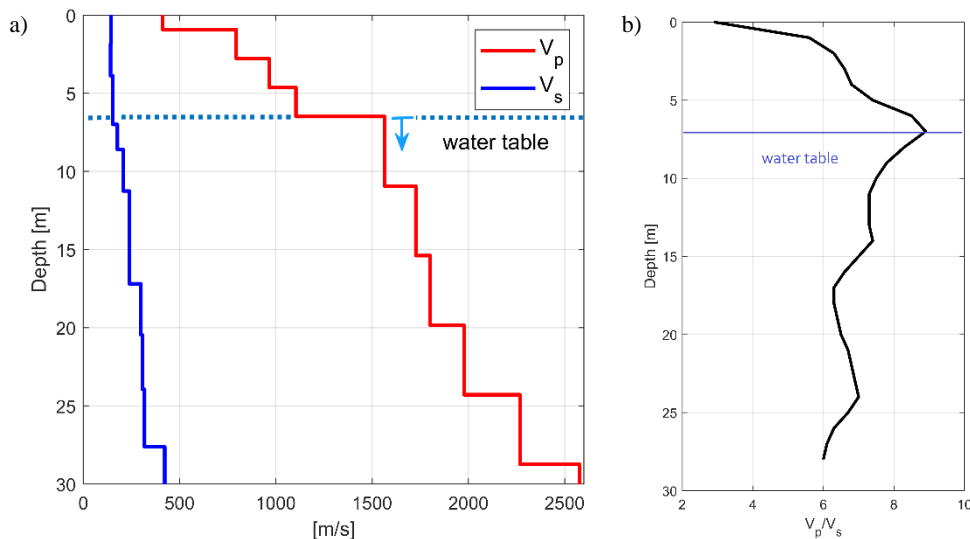


Fig. 14 (a) 1D V_p and V_s models (red and blue bold line respectively) with a water table level (blue dashed line); (b) V_p/V_s ratio with a water table level (blue line).

according to the nearby borehole JS-186 consists of six meters of weathered rock and soil on the top followed by a one-meter-thick clay layer, then ten meters of gravel and gravel sands and from a depth of 17 m the clay predominates.

In order to establish the parameter V_{s30} we acquired vertical component of Rayleigh waves (Fig. 13) and standard V_p refraction tomography data (Fig. 12). For that purpose, 4.5 Hz vertical geophones with three meters spacing (Fig. 13a) were used with a 10 kg sledgehammer as an active source. Shot gathers data (Figs. 13b and c) were processed in a standard MASW scheme – a dispersion images (Figs. 13d and e) were obtained using a phase shift transformation, and R_w fundamental mode dispersion curves from two shots on both ends of the profile were inverted using LSM to get the average V_s model (Fig. 14a).

Refraction data were processed to a 2D travel time tomography model (Fig. 12) and a 1D V_p model was retrieved from the middle part of the tomography profile and plotted together with the 1D V_s model (Fig. 14a) from the dispersion analysis. From the nearby borehole JS-186 we were able to obtain a water table values (blue dashed line in Figure 14a). Correlation of hydrogeological data with V_p and V_s models in Figure 14a shows that there is a significant V_p increase in the water table depth. Figure 14b displays V_p/V_s ratio together with the hydrogeological data and shows that water table is characterized in the seismic velocity plot as a peak with the maximum V_p/V_s ratio reaching values over eight. A generally high V_p/V_s is to be expected here, Barton (2006) even observed values between 20 to 40 in the case of unconsolidated sediments. Both observations are consistent with the assumption that the velocity of shear waves increases much less than the velocity of compressional waves in saturated soils, as declared e.g., in Grelle and Guadagno (2009).

CASE STUDY 4

In the previous case studies, we have presented possibilities offered by dispersive analysis of surface waves obtained by active acquisition during a conventional refraction seismic survey. In the Case study 4 we demonstrate how the active data can be effectively supplemented with an additional independent observation – a passive noise monitoring. The passive (ambient) MASW represents an additional independent dataset that can be effectively acquired in a short time without any further effort using the identical geometry of refraction receiver spread used for the tomography or active MASW. Passively acquired surface waves generated from natural or cultural sources are usually of a low-frequency nature (1–20 Hz) and therefore provides information from depths that the active data is missing (Tokimatsu et al., 1992a; Park and Miller, 2005). In a subsequent joint analysis passively obtained dataset covers the low-frequency end of a dispersion curve and provides information from deeper parts of the environment whereas active data covers the higher frequency related to the subsurface layers. As stated in Park et al. (2007) this can result in a combined active-passive analysis of surface waves to obtain both shallow (e.g., 1–20 m) and deep (e.g., 20–100 m) V_s information simultaneously and thus can significantly increase the depth reach of the survey.

The data of Case study 4 (Fig. 15) were collected in NW-Czechia in the vicinity of the seismic station Skalica (SKAC) – a part of the RINGEN seismic monitoring network (Fischer et al., 2023; Káldy and Fischer, 2023). The site is situated in the Bohemian Cretaceous Basin within the Merboltice formation (Šafanda et al., 2020). Data were acquired using 24x 4.5Hz vertical geophones (Fig 16. for tomography, active and passive MASW) with 4 m spacing and a 10 kg sledgehammer as an active seismic source. When the active data were acquired, the same geometry was used for a 20 min passive acquisition.

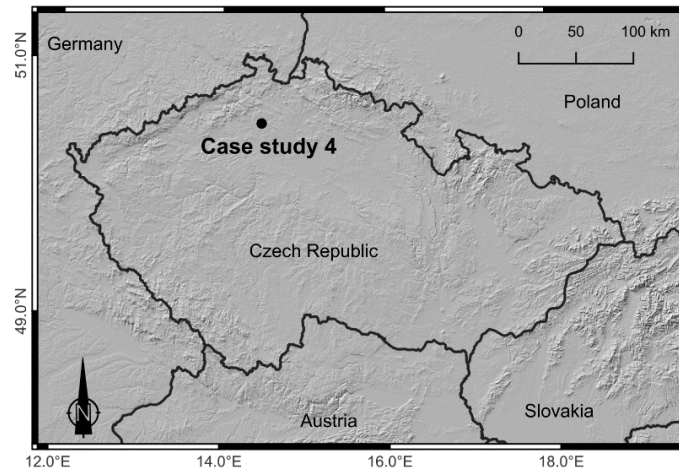


Fig. 15 Case study 4 site map.

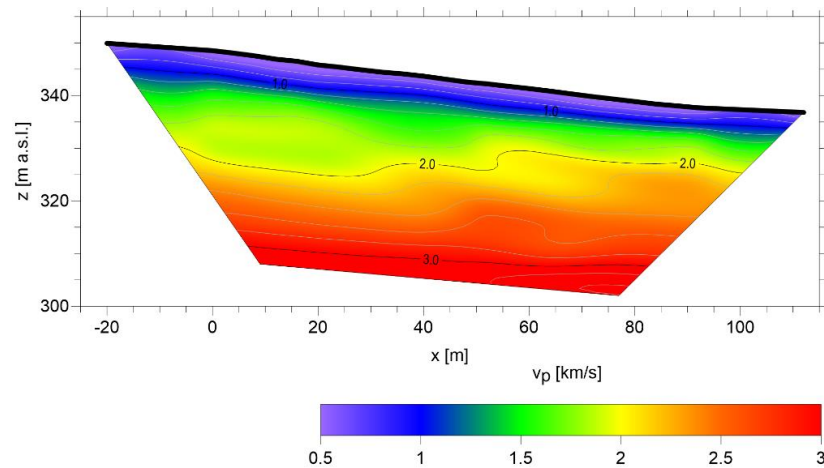


Fig. 16 P-wave travel time tomography model of the SKAC site.

Figure 16 shows the travel time tomography profile suggesting that the geological environment could be considered 1D. To reduce the uncertainty of the tomography by increasing the number of observables, a dispersion analysis of surface waves was carried out (Fig. 17). The active MASW data were analysed in a standard way using the Phase shift method and picking the fundamental mode (Figs. 17 b and d). The passive data were transformed using SPAC (Figs. 17 c and e). For the inversion analysis the experimental dispersion curve was compiled from both active and passive dispersion curves. As shown in Figure 18b the low frequency part of the dispersion curve was constructed from the passive data whereas the high frequencies were defined by the active data processing.

The resulting V_s model of the joint inversion of the passive and active MASW Rayleigh wave phase velocity is displayed in Figure 18a. The V_s model is generally consistent with the tomography model

(Fig. 16). In the shallowest part, both show low seismic velocities corresponding to clays and the near-surface weathered zone. A significant velocity increase is visible in both models at the depths of approximately 18 m and 30 m. Both probably corresponding to lithological changes in a sedimentary sequence. However, in the tomography model the deeper interface is very close to the bottom depth limit of the survey and hence the long-period components of the surface waves proving reliability of the resolved velocity model are extremely valuable. As the V_s model in Figure 18 shows there is very likely a significant interface (high velocity increase) at a depth of about 44 m that beyond the depth reach of the tomography. The last interpreted interface could represent a lithological change (to coarser and stiffer layers) in the Cretaceous sedimentary sequence. Unfortunately, due to the lack of relevant boreholes with adequate depth in the area we can only speculate about this explanation.

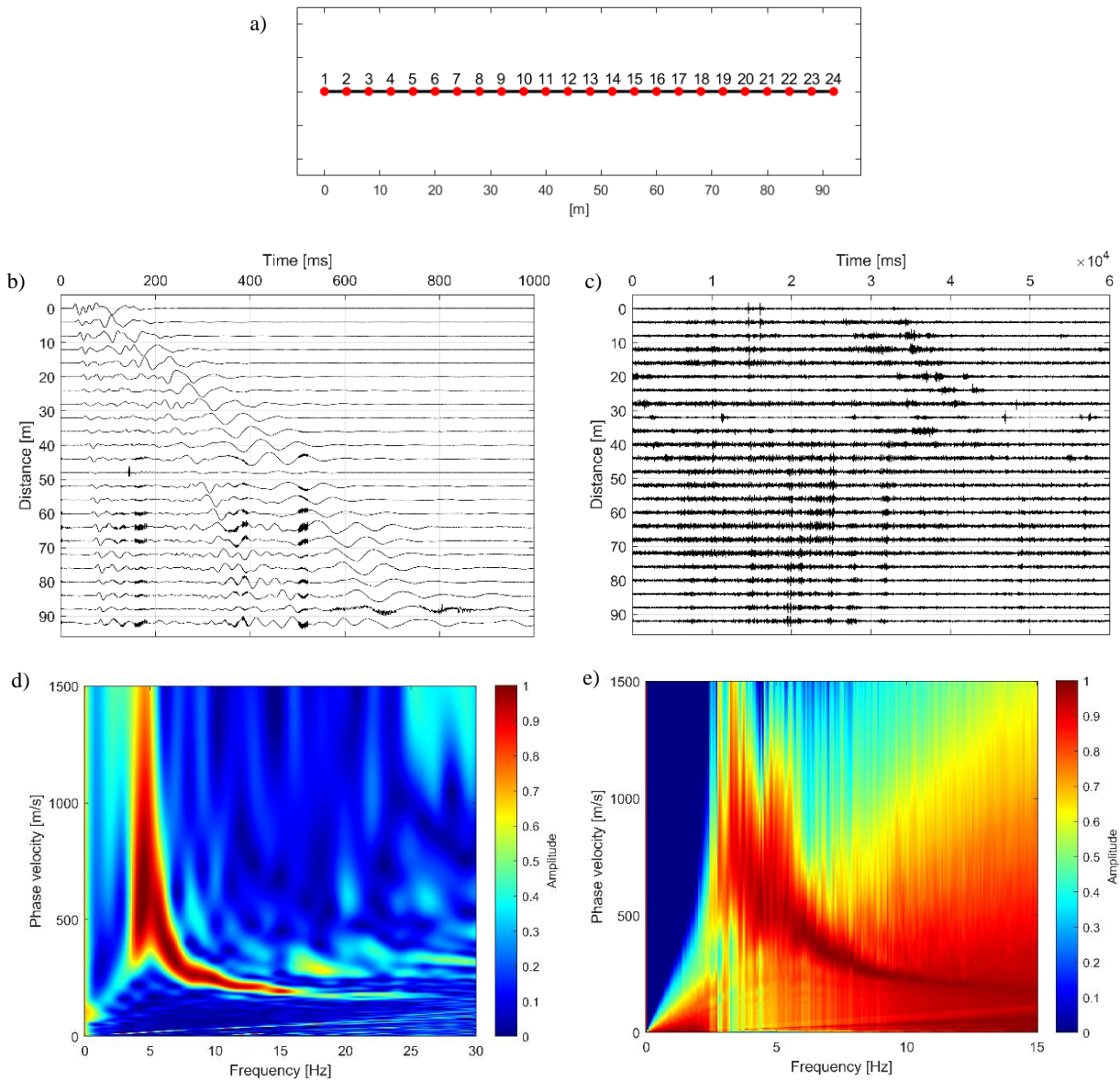


Fig. 17 (a) Geophone array geometry of the SKAC site; (b) active data shot gather from the -10 m source position; (c) 60 s passive MASW seismic traces; (d) active data dispersion spectra (e) passive data dispersion spectra.

DISCUSSION

Surface waves analysis and especially MASW is one of the easiest seismic methods that provides highly favourable S/N data, and therefore is more tolerant in parameter selection than any other seismic methods (Park et al., 2007). Furthermore, the MASW makes it cost and time effective to evaluate shear wave velocity in one, two (or three) dimensions (e.g., Olafsdotir, 2016). A significant advantage is that this method can be generally used as a complementary method to standard seismic refraction. Both methods involve the estimation of subsurface velocity profiles. MASW estimates the shear wave velocity (V_s) profile using the dispersion characteristics of surface waves, while seismic refraction estimates the seismic velocity (P-wave or S-wave) profile by measuring the travel

times of refracted waves. If the refraction acquisition meets the above listed MASW acquisition requirements (low frequency geophones, appropriate source offset, etc.), surface wave dispersion analysis can be performed on the same dataset. Thus, the output can be P-wave (e.g., from refraction tomography) and S-wave (retrieved from surface waves analysis) velocity models. These two observables complement each other since both P and S-waves are sensitive to different parameters of the rock environment (e.g., Barton, 2006) and both are retrieved from different methods/principles. Therefore, using surface waves analysis can reduce the non-uniqueness of the solution and help to better constrain the subsurface model. Both MASW and seismic refraction however require careful consideration of site-specific factors such as

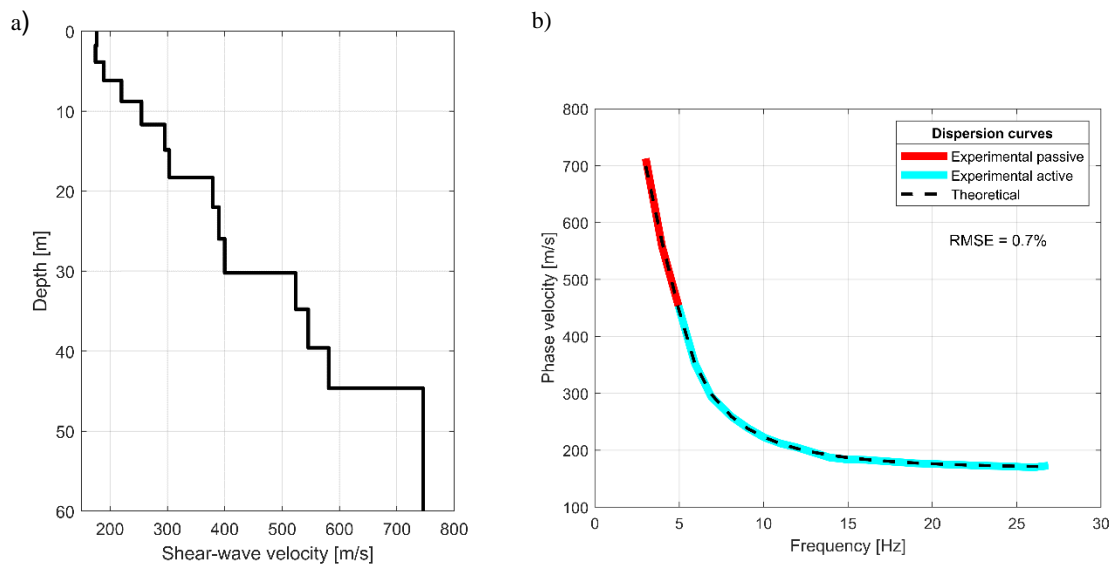


Fig. 18 Result of the joint inversion of the passive and active MASW Rayleigh wave phase velocity (a) retrieved Vs model and (b) related experimental (red bold line shows the part of the joint dispersion curve that was derived dominantly from passive data and blue line represents active MASW data) and theoretical (dashed line) dispersion curves and inversion RMSE.

geologic conditions, surface topography, and acquisition parameters to ensure accurate and reliable results. Proper data acquisition and analysis are crucial for both methods to obtain reliable subsurface information.

In this study we illustrated on four case studies how inclusion of basic surface waves analysis into the standard refraction survey could decrease the ambiguity of solution and extend the obtained knowledge at no additional cost. By comparison of 4.5 and 10 Hz geophone data (Figs. 5 and 6) in Case study 1 we illustrated that it may be beneficial to incorporate surface wave dispersive analysis into the standard shallow refraction seismic process as a convenient complement requiring no additional equipment, data, or effort. We do not deny that low-frequency geophones are more suitable for surface waves dispersion analysis and allows to get information from deeper parts of environment. However, the lack of low-frequency geophones should not be a reason to reject this type of analysis, although it must be carried out with caution (Dean and Shem, 2018). Case study 2 demonstrated that additional MASW analysis (Figs. 9 and 10) of refraction data can provide information about substantial changes in elastic properties of the subsurface, in this case velocity interfaces, not revealed by conventional tomography. In Case study 3 we showed that retrieving V_p and V_s from a single acquisition setup (Figs. 12 and 13) appears attractive in terms of time and equipment costs and can effectively provide supplementary information and expand the understanding of aquifer systems in accordance with Konstantaki et al. (2013) and Pasquet et al. (2015). In Case study 4 we pointed

out that adding a passive MASW in the standard refraction scheme is virtually effortless (consumes only $\sim +20$ min) and can expand the penetration depth and add independent observable. Passive MASW data can be included in joint analysis with active MASW to obtain both shallow and deep Vs as we showed in Figure 18. This survey mode can be useful and convenient because of the significant advantage in field operations and coverage of wide range of wavelength components of Rayleigh waves (Park et al., 2007).

Nevertheless, as any geophysical methods, the MASW has inevitable drawbacks. Dal Moro (2023) discussed the main shortcomings of this method and especially warned that: (1) the standard MASW approach is based on the personal (i.e., subjective) interpretation of the Rayleigh waves phase-velocity spectrum and (2) even in case data interpretation is correct, non-uniqueness of the solution obtained from inversion of just one observable remains a problem. The latter is also related to risk of lateral variations that can produce complex or meaningless velocity spectra. Author further highlighted the need for multi-component analysis to overcome the ambiguities of single-component analysis.

However, as the presented case studies show, even the simple MASW yields realistic results, if only the dispersion analysis of surface waves is performed carefully and the limitations are considered and obeyed. This includes especially the need to determine the shear wave velocity model only at depths corresponding to the intelligible part of the dispersion curve(s) and careful discrimination of individual modes.

CONCLUSIONS

Surface waves analysis and especially MASW is a valuable and cost-effective seismic method for subsurface characterization. It has a wide range of applications and can provide useful information about the shear wave velocity profile. As we showed in four case studies significant advantage is that this method can be generally used as a complementary method to seismic refraction. It can expand the observables in a short time and with minimum effort. This can result in multi-objective joint analysis useful in e.g., geotechnical (Case study 2 and 4) and hydrogeological (Case study 3) studies and significantly decrease the ambiguity of solution. However, it is important to bear in mind its limitations and challenges, (as listed above). Proper data acquisition and analysis should be employed, and it is recommended to integrate MASW with other approaches and/or objectives and geological information for a comprehensive understanding of the subsurface. When used properly and with an understanding of its limitations MASW can be a powerful tool for subsurface investigation in various geological and geotechnical settings and can significantly expand the knowledge derived from the refraction data. It can also serve for practitioners as an introduction to surface waves analysis and can motivate them for further study in this field.

ACKNOWLEDGEMENT

This study was supported by the Charles University Grant Agency (GA UK) nr. 576120 and Technology Agency of the Czech Republic, project TK03010160.

REFERENCES

- Abudeif, A.M., Fat-Helbary, R.E., Mohammed, M.A., Alkhashab, H.M. and Masoud, M.M.: 2019, Geotechnical engineering evaluation of soil utilizing 2D multichannel analysis of surface waves (MASW) technique in New Akhmim city, Sohag, Upper Egypt. *J. African Earth Sci.*, 157, 2, 103512. DOI: 10.1016/j.jafrearsci.2019.05.020
- Aki, K.: 1957, Space and time spectra of stationary stochastic waves, with special reference to microtremors. *Bull. Earthq. Res. Inst.*, 35, 415–456.
- Bachrach, R., Dvorkin, J. and Nur, A.M.: 2000, Seismic velocities and Poisson's ratio of shallow unconsolidated sands. *Geophysics*, 65, 2, 559–564. DOI: 10.1190/1.1444751
- Barton, N.: 2006, Rock quality, seismic velocity, attenuation and anisotropy. CRC Press, 729 pp. DOI: 10.1201/9780203964453
- Dal Moro, G.: 2014, Surface wave analysis for near surface applications. Elsevier, Amsterdam, The Netherlands, 252 pp. DOI: 10.1007/978-3-030-46303-8
- Dal Moro, G.: 2020, Efficient joint analysis of surface waves and introduction to vibration analysis: beyond the clichés. Springer, Nature. DOI: 10.1007/978-3-030-46303-8
- Dal Moro, G.: 2023, MASW? A critical perspective on problems and opportunities in surface-wave analysis from active and passive data (with few legal considerations). *Phys. Chem. Earth*, 130, 103369. DOI: 10.1016/j.pce.2023.103369
- Dal Moro, G. and Ferigo, F.: 2011, Joint analysis of Rayleigh-and Love-wave dispersion: Issues, criteria and improvements. *J. Appl. Geophys.*, 75, 3, 573–589. DOI: 10.1016/j.jappgeo.2011.09.008
- Dal Moro, G., Pipan, M., Forte, E. and Finetti, I.: 2003, Determination of Rayleigh wave dispersion curves for near surface applications in unconsolidated sediments. Proc. SEG International Exposition and 73rd Annual Meeting, 24-31 October 2003, Dallas, Texas, 22, 1247–1250.
- Dean, T. and Shem, A.: 2018, Methods for reducing unwanted noise (and increasing signal) in passive seismic surveys. ASEG Extended Abstracts, 1, 1–7. DOI: 10.1071/ASEG2018abW8_2A
- Debeglia, N., Bitri, A. and Thierry, P.: 2006, Karst investigations using microgravity and MASW: Application to Orléans, France. *Near Surf. Geophys.*, 4, 4, 215–225. DOI: 10.3997/1873-0604.2005046
- Evison, F.F., Ingham, C.E., Orr, R.A. and Le Fort, J.H.: 1960, Thickness of the Earth's crust in Antarctica and the surrounding oceans. *Geophys. J. Int.* 3, 3, 289–306. DOI: 10.1111/J.1365-6X.1960.TB01704.X
- Fischer, T., Vlček, J., Dědeček, P., Řihošek, J., Zimmermann, G., Holeček, J., Mazanec M., Rukavičková, L., Janků, L. and Káldy, E.: 2023, Hydraulic injection tests in the pilot EGS borehole PVGT-LT1 in Litoměřice, Czechia. *Geothermics*, 115, 102805. DOI: 10.1016/j.geothermics.2023.102805
- Foti, S., Parolai, S., Bergamo, P., Di Giulio, G., Maraschini, M., Milana, G., ... and Puglia, R.: 2011, Surface wave surveys for seismic site characterization of accelerometric stations in ITACA. *Bull. Earthq. Eng.*, 9, 1797–1820. DOI: 10.1007/s10518-011-9306-y
- Foti, S., Lai, C., Rix, G.J. and Strobbia, C.: 2014, Surface wave methods for near-surface site characterization (1st ed.). CRC Press. DOI: 10.1201/b17268
- Foti, S., Hollender, F., Garofalo, F., Albarello, D., Asten, M., Bard, P.Y., ... and Socco, V.: 2018, Guidelines for the good practice of surface wave analysis: a product of the InterPACIFIC project. *Bull. Earthq. Eng.*, 16, 2367–2420. DOI: 10.1007/s10518-017-0206-7
- Gabriels, P., Snieder, R. and Nolet, G.: 1987, In situ measurements of shear wave velocity in sediments with higher mode Rayleigh waves. *Geophys. Prospect.*, 35, 2, 187–196. DOI: 10.1111/j.1365-2478.1987.tb00812.x
- Gaytan, A.R., Estrella, H.F., Preciado, A., Bandy, W.L., Lazcano, S., Nolasco, L.A., ... and Korn, M.: 2020, Subsoil classification and geotechnical zonation for Guadalajara City, México: Vs30, soil fundamental periods, 3D structure and profiles. *Near Surf. Geophys.*, 18, 2, 175–188. DOI: 10.1002/nsg.12085
- Grelle, G. and Guadagno, F.M.: 2009, Seismic refraction methodology for groundwater level determination: “Water seismic index”. *J. Appl. Geophys.*, 68, 3, 301–320. DOI: 10.1016/j.jappgeo.2009.02.001
- Hayashi, K., Asten, M.W., Stephenson, W.J., Cornou, C., Hobiger, M., Pilz, M. and Yamanaka, H.: 2022, Microtremor array method using spatial autocorrelation analysis of Rayleigh-wave data. *J. Seismol.*, 26, 4, 601–627. DOI: 10.1007/s10950-021-10051-y

- Hollender, F., Cornou, C., Dechamo, A., Oghalaei, K., Renalier, F., Maufroy, E. et al.: 2018, Characterization of site conditions (soil class, VS30, velocity profiles) for 33 stations from the French permanent accelerometric network (RAP) using surface wave methods. *Bull. Earthq. Eng.*, 16, 2337–2365. DOI: 10.1007/s10518-017-0135-5
- Jongmans, D. and Demanet, D.: 1993, The importance of surface waves in vibration study and the use of Rayleigh waves for estimating the dynamic characteristics of soils. *Eng. Geol.*, 34, 1-2, 105–113. DOI: 10.1016/0013-7952(93)90046-F
- Joniak, P., Šujan, M., Fordinál, K., Braucher, R., Rybár, S., Kováčová, M., ... and Keddadouche, K.: 2020, The age and paleoenvironment of a late Miocene floodplain alongside Lake Pannon: Rodent and mollusk biostratigraphy coupled with authigenic $^{10}\text{Be}/^9\text{Be}$ dating in the northern Danube Basin of Slovakia. *Palaeogeogr. Palaeoclimatol. Palaeoecol.*, 538, 109482. DOI: 10.1016/j.palaeo.2019.109482
- Káldy, E. and Fischer, T.: 2023, Microseismic network sensitivity in case of no seismic activity: Case study from Litoměřice in Czech Republic, proof-tested in West Bohemia. *J. Seismol.*, 1606, 15. DOI: 10.1007/s10950-023-10134-y
- Kanlı, A.I., Tildy, P., Prónay, Z., Pınar, A. and Hermann, L.: 2006, VS 30 mapping and soil classification for seismic site effect evaluation in Dinar region, SW Turkey. *Geophys. J. Int.*, 165, 1, 223–235. DOI: 10.1111/j.1365-246X.2006.02882.x
- Kaufmann, R.D., Xia, J., Benson, R.C., Yuhr, L.B., Casto, D.W. and Park, C.B.: 2005, Evaluation of MASW data acquired with a hydrophone streamer in a shallow marine environment. *J. Environ. Eng. Geophys.*, 10, 2, 87–98. DOI: 10.2113/JEEG10.2.87
- Knopoff, L. and Panza, G.P.: 1977, Resolution on upper mantle structure using higher modes of Rayleigh waves. *Ann. Geophys.*, 30, 3-4, 491–505.
- Kolínský, P., Valenta, J. and Málek, J.: 2014, Velocity model of the Hronov-Poříčí Fault Zone from Rayleigh wave dispersion. *J. Seismol.*, 18, 617–635. DOI: 10.1007/s10950-014-9433-4
- Konstantaki, L.A., Carpentier, S., Garofalo, F., Bergamo, P. and Socco, L.V.: 2013, Determining hydrological and soil mechanical parameters from multichannel surface wave analysis across the Alpine Fault at Incheon, New Zealand. *Near Surf. Geophys.*, 11, 4, 435–448. DOI: 10.3997/1873-0604.2013019
- Lai, C.G.: 1998, Simultaneous inversion of Rayleigh phase velocity and attenuation for near surface site characterization. Ph.D Thesis. Georgia Institute of Technology.
- Lai, C.G., Mangriotis, M.D. and Rix, G.J.: 2014, An explicit relation for the apparent phase velocity of Rayleigh waves in a vertically heterogeneous elastic half-space. *Geophys. J. Int.*, 199, 2, 673–687. DOI: 10.1093/gji/ggu283
- Lin, C.P., Chang, C.C. and Chang, T.S.: 2004, The use of MASW method in the assessment of soil liquefaction potential. *Soil Dyn. Earthq. Eng.*, 24, 9, 689–698. DOI: 10.1016/j.soildyn.2004.06.012
- McMechan, G.A. and Yedlin, M.J.: 1981 Analysis of dispersive waves by wave field transformation. *Geophysics*, 46, 6, 869–874. DOI: 10.1190/1.1441225
- Miller, R.D., Xia, J., Park, C.B. and Ivanov, J.M.: 1999, Multichannel analysis of surface waves to map bedrock. *Lead. Edge*, 18, 1392–1396. DOI: 10.1190/1.1438226
- Odum, J.K., Stephenson, W.J., Williams, R.A. and von Hillebrandt Andrade, C.: 2013, VS30 and spectral response from collocated shallow, active and passive source VS data at 27 sites in Puerto Rico. *Bull. Seismol. Soc. Am.*, 103, 5, 2709–2728. DOI: 10.1785/0120120349
- Ohori, M., Nobata, A. and Wakamatsu, K.: 2002, A comparison of ESAC and FK methods of estimating phase velocity using arbitrarily shaped microtremor arrays. *Bull. Seismol. Soc. Am.*, 92, 2323–2332. DOI: 10.1785/0119980109
- Olafsdottir, E.A.: 2016, Multichannel analysis of surface waves for soil site characterization. Ph.D. Thesis, University of Iceland, Reykjavik, Iceland.
- Park, C.: 2013, MASW for geotechnical site investigation. *Lead. Edge*, 32, 6, 656-662. DOI: 10.1190/1.1432060656.1
- Park, C.: 2016, MASW analysis of bedrock velocities (V_s and V_p). 86th Ann. Mtg. SEG, October 16-21, 2016, Dallas, Texas. DOI: 10.1190/segam2016-13778114.1
- Park, C.B. and Carnevale, M.: 2010, Optimum MASW survey-revisit after a decade of use. In: *Proc. GeoFlorida Conference 2010: Advances in Analysis, Modeling and Design*. American Society of Civil Engineers, Orlando, 1303–1312. DOI: 10.1061/41095(365)130
- Park, C.B. and Miller, R.D.: 2005, Multichannel analysis of passive surface waves— modeling and processing schemes. *Proc. Geo-Frontiers conference*, Austin, Texas, January 23-26.
- Park, C.B., Miller, R.D. and Xia, J.: 1998, Imaging dispersion curves of surface waves on multi-channel record. 68th Annual International Meeting Society Exploration Geophysics, Expanded Abstracts, 377–1380. DOI: 10.1190/1.1820161
- Park, C.B., Miller, R.D. and Xia, J.: 1999, Multichannel analysis of surface waves. *Geophysics*, 64, 800–808. DOI: 10.1190/1.1444590
- Park, C.B., Miller, R.D. and Miura, H.: 2002, Optimum field parameters of an MASW survey. *Proc. 6th SEG-J International Symposium*, Tokyo, Japan, 22–23 May 2002.
- Park, C., Miller, R., Laflen, D., Bennett, B., Ivanov, J., Neb, C. and Huggins, R.: 2004, Imaging dispersion curves of passive surface waves. In: *SEG International Exposition and Annual Meeting*. DOI: 10.1190/1.1851112
- Park, C.B., Miller, R.D., Xia, J. and Ivanov, J.: 2007, Multichannel analysis of surface waves (MASW) - active and passive methods. *Lead. Edge*, 26, 1, 60–64. DOI: 10.1190/1.2431832
- Pasquet, S., Bodet, L., Dhemaied, A., Mouhri, A., Vitale, Q., Rejiba, F., ... and Guérin, R.: 2015, Detecting different water table levels in a shallow aquifer with combined P-, surface and SH-wave surveys: Insights from VP/VS or Poisson's ratios. *J. Appl. Geophys.*, 113, 38–50. DOI: 10.1016/j.jappgeo.2014.12.005
- Penumadu, D. and Park, C.B.: 2005, Multichannel analysis of surface wave (MASW) method for geotechnical site characterization. *Proc. GeoFrontiers 2005: Earthquake Engineering and Soil Dynamics*. DOI: 10.1061/40779(158)3

- Rahman, M.Z., Kamal, A.M. and Siddiqua, S.: 2018, Near-surface shear wave velocity estimation and Vs30 mapping for Dhaka City, Bangladesh. *Nat. Hazards*, 92, 1687–1715. DOI: 10.1007/s11069-018-3266-3
- Ritzwoller, M.H. and Levshin, A.L.: 1998, Eurasian surface wave tomography: Group velocities. *J. Geophys. Res., Solid Earth*, 103, 4839–4878. DOI: 10.1029/97JB02622
- Šafanda, J., Verner, K., Franěk, J., Peřestý, V., Holeček, J. and Fischer, T.: 2020, Geology and geothermal potential in the eastern flank of Eger Rift (Litoměřice area, Czech Republic). *Geothermics*, 86, 101808. DOI: 10.1016/j.geothermics.2020.101808
- Sairam, B., Singh, A.P., Patel, V., ... and Ravi, Kumar, M.: 2019, VS30 mapping and site characterization in the seismically active intraplate region of Western India: implications for risk mitigation. *Near Surf. Geophys.*, 17, 5, 533–546. DOI: 10.1002/nsg.12066
- Socco, L.V., Foti, S. and Boiero, D.: 2010, Surface-wave analysis for building near-surface velocity models - Established approaches and new perspectives. *Geophysics*, 75, 5. DOI: 10.1190/1.3479491
- Strelec, S., Mesec, J., Grabar, K. and Jug, J.: 2017, Implementation of in-situ and geophysical investigation methods (ERT & MASW) with the purpose to determine 2D profile of landslide. *Acta Montan. Slovaca*, 22, 4.
- Stümpel, H., Kähler, S., Meissner R. and Milkereit, B.: 1984, The use of seismic shear waves and compressional waves for lithological problems of shallow sediments. *Geophys. Prospect.*, 32, 4, 662–675.
- Suto, K.: 2012, An application of multi-channel analysis of surface waves (MASW) to hydrological study: A case history. *ASEG Extended Abstracts*, 1, 1-4. DOI: 10.1071/ASEG2012ab044
- Suto, K., Urošević, M. and Komatina, S.: 2016, An MASW survey for landslide risk assessment: A case study in Valjevo, Serbia. *Chiang. Mai J. Sci.*, 43, 6, 1240–1258.
- Turesson, A.: 2007, A comparison of methods for the analysis of compressional, shear, and surface wave seismic data, and determination of the shear modulus. *J. Appl. Geophys.*, 61, 2, 83–91. DOI: 10.1016/j.jappgeo.2006.04.005
- Tokimatsu, K., Shinzawa, K. and Kuwayama, S.: 1992a, Use of short-period microtremors for Vs profiling. *J. Geotech. Eng., ASCE*, 118, 10, 1544–1558. DOI:10.1061/(ASCE)0733-9410(1992)118:10(1544)
- Tokimatsu, K., Tamura, S. and Kojima, H.: 1992b, Effects of multiple modes on Rayleigh wave dispersion characteristics. *J. Geotech. Eng., ASCE*, 118, 10, 1529–1543. DOI: 10.1061/(ASCE)0733-9410(1992)118:10(1529)
- Vavryčuk, V.: 2008, Velocity, attenuation, and quality factor in anisotropic viscoelastic media: A perturbation approach. *Geophysics*, 73, D63–D73. DOI: 10.1190/1.2921778
- Xia, J., Miller, R.D. and Park, C.B.: 1999, Estimation of near-surface shear-wave velocity by inversion of Rayleigh waves. *Geophysics*, 64, 3, 691–700. DOI: 10.1190/1.1444578
- Xia, J., Miller, R.D., Park, C.B., Hunter, J.A., Harris, J.B. and Ivanov, J.: 2002, Comparing shear-wave velocity profiles inverted from multichannel surface wave with borehole measurements. *Soil Dyn. Earthq. Eng.*, 22, 3, 181–190. DOI: 10.1016/S0267-7261(02)00008-8
- Yilmaz, Ö.: 1987, Seismic data processing. Society of Exploration Geophysicists, Tulsa, OK, pp. 526.
- Zhou, L., Song, X., Yang, X. and Zhao, C.: 2020, Rayleigh wave attenuation tomography in the crust of the Chinese Mainland. *Geochemistry Geophys. Systems*, 21, e2020GC008971. DOI: 10.1029/2020GC008971